Electronic Supplementary Information

Asymmetric donor-acceptor-host red thermally activated delayed fluorescent emitter for high-efficiency organic light emitting diodes

Hao-Ze Li,[a] Feng-Ming Xie,*,[b] Ping Wu,[c] Kai Zhang,[d] Xin Zhao,*,[c] Yan-Qing Li,*,[a] Jian-Xin Tang*,[b,d]

[a] *School of Physics and Electronic Science, East China Normal University, Shanghai 200062 (P. R. China)*

[b] *Jiangsu Key Laboratory for Carbon-Based Functional Materials & Devices, Institute of Functional Nano & Soft Materials (FUNSOM), Soochow University, Suzhou, Jiangsu 215123 (P. R. China)*

[c] *School of Chemistry and Life Sciences, Suzhou University of Science and Technology, Suzhou, Jiangsu 215009 (P. R. China)*

[d] *Macao Institute of Materials Science and Engineering (MIMSE), Faculty of Innovation Engineering, Macau University of Science and Technology, Taipa, Macao 999078 (P. R. China)*

E-mail: fmxie@suda.edu.cn (F.-M. Xie), zhaoxin_sz@mail.usts.edu.cn (X. Zhao), yqli@phy.ecnu.edu.cn (Y.-Q. Li), jxtang@suda.edu.cn (J.-X. Tang)

Experimental Section

Chemical Synthesis: All the reagents were purchased from commercial sources, and were not purified. All the reactions were carried out in a nitrogen atmosphere, and the crude product was purified by column chromatography before material properties and device manufacture.

Materials Characterization: ^{1}H-NMR was recorded at room temperature with a Bruker AVANCE III type NMR Spectrometer in CDCl$_3$ solution, and ultrafleXtreme MALDI-TOF mass spectrometer. The UV-Vis absorption and photoluminescence spectra of the emitter were measured with the concentration of 10 $^{-5}$ mol L^{-1}. The thermal decomposition temperature (5% mass loss) of the three emitters were measured by an HCT-2 thermogravimetric analyzer. Thermogravimetric analysis curves were measured under nitrogen atmosphere with a heating rate of 10 °C/min and range of 50-800 °C. The electrochemical properties of the emitter were performed by cyclic voltammetry (CV) on the RST 3100 electrochemical workstation. The UV-Vis absorption spectra were processed on a Perkin-Elmer Lambda 750 UV-Vis spectrophotometer. The fluorescence spectra and low-temperature phosphorescence spectra were measured at 77 K a FM-4 type fluorescence spectrophotometer (JY company, French). PLQY of **TPA-AQ-DCP** was measured the films were measured using an absolute PLQY spectrometer (C9920-02G, Hamamatsu Photonics, Japan) at room temperature under nitrogen atmosphere. Temperature-dependent transient PL decay measurements were conducted using a Quantaurus-Tau fluorescence lifetime spectrometer (C11367-01, Hamamatsu Photonics, Japan) and a cryostat (Oxford Instruments) with an excitation wavelength of 373 nm under a vacuum.

OLED fabrication and measurements: The ITO glass must be cleaned to remove impurities from the surface. The organic materials and metal electrodes required for the OLED device must be put into the evaporator template for vacuum evaporation with vacuum degree below 2×10^{-4} Pa, the organic layer is 2-3 Å/s, the Liq layer deposition rate is 0.1 Å/s, and the Al deposition rate is > 6 Å/s. After the deposition, the devices need to be cooled and encapsulated by UV curing glue. The electroluminescence characteristics of OLEDs device were measured by a source meter (Keithley Model

2400) and a luminance meter/spectrometer (PhotoResearch PR655).

General information

The solvents used and the raw materials for synthesis were from commercial sources and directly used without any further purification.

Synthesis of TPA-AQ-DCP
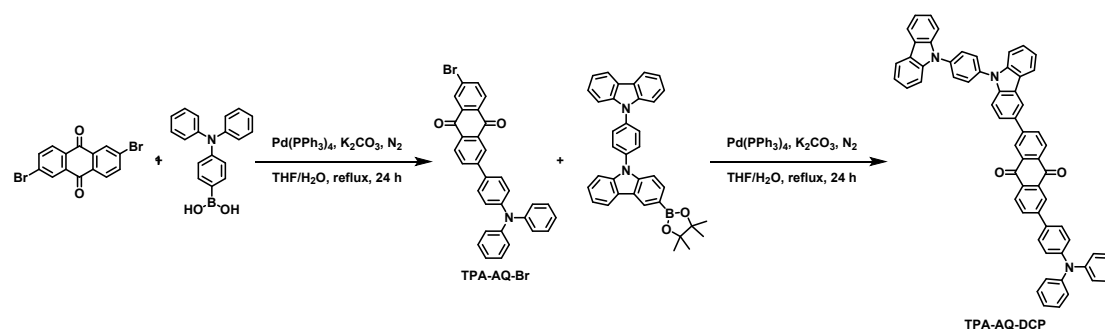
Scheme S1. Synthetic routes of **TPA-AQ-DCP**.

2,6-dibromoanthracene-9,10-dione (0.51 g, 1.38 mmol), (4-(diphenylamino)phenyl)boronic acid (0.34 g, 1.18 mmol) and potassium carbonate (0.9682 g, 7.01 mmol) were dissolved into 50 ml mixed solution (THF: H_2O=5:1). Under the nitrogen atmosphere, the reactants were stirred for 5 minutes. Then tetrakis(triphenylphosphine)palladium (5% equi) was added to the mixed solution, the reaction temperature was adjusted to 70°C, and the mixture was stirred at reflux for 12 hours. After the mixed solution was cooled to room temperature, it was poured into NaOH aqueous solution and stirred, and the precipitated red solid was collected by vacuum filtration. It was further purified by silica gel column chromatography (DCM:PE=1:3) to obtain 0.40 g of red powder (2-bromo-6-(4-(diphenylamino)phenyl)anthracene-9,10-dione, TPA-AQ-Br) (yield 64%). MALDI-TOF-MS (m/z) of $C_{32}H_{20}BrNO_2$ for $[M]^+$: 529.068; Found: 528.905.

The TPA-AQ-Br (0.4 g, 0.75 mmol) and 9-(4-(9H-carbazol-9-yl)phenyl)-3-(4,4,5,5-tetramethyl-1,3,2-dioxaborolan-2-yl)-9H-carbazole (0.45 g, 0.85 mmol) were added into a three neck flask. The following drugs were added to the reaction flask under nitrogen protection: 30 mL THF, 6 mL H_2O, 0.82 g potassium carbonate and 5%

equivalent of tetrakis(triphenylphosphine)palladium. After heating and stirring at 70 °C for 24 hours, the reaction mixture was cooled to room temperature. The reaction solution was poured into 100 mL water, extracted with DCM (30 mL×3), and the organic phase was concentrated. The final purification yielded 0.35 g (54% yield) of orange-red powder (**TPA-AQ-DCP**). ^{1}H NMR (400 MHz, CDCl$_3$) δ 8.75 (s, 1H), 8.59 (s, 2H), 8.46 (dd, J = 18.4, 8.0 Hz, 2H), 8.32 (d, J = 7.7 Hz, 1H), 8.23 (d, J = 7.6 Hz, 2H), 8.04 (d, J = 8.0 Hz, 1H), 7.90 (s, 4H), 7.65 (dd, J = 19.1, 8.3 Hz, 6H), 7.53 (d, J = 7.4 Hz, 3H), 7.35 (dd, J = 16.6, 8.4 Hz, 9H), 7.21 (t, J = 6.2 Hz, 6H), 7.12 (s, 2H). MALDI-TOF-MS (m/z) of C$_{62}$H$_{39}$N$_3$O$_2$ for [M]$^+$: 857.304; Found: 857.254.
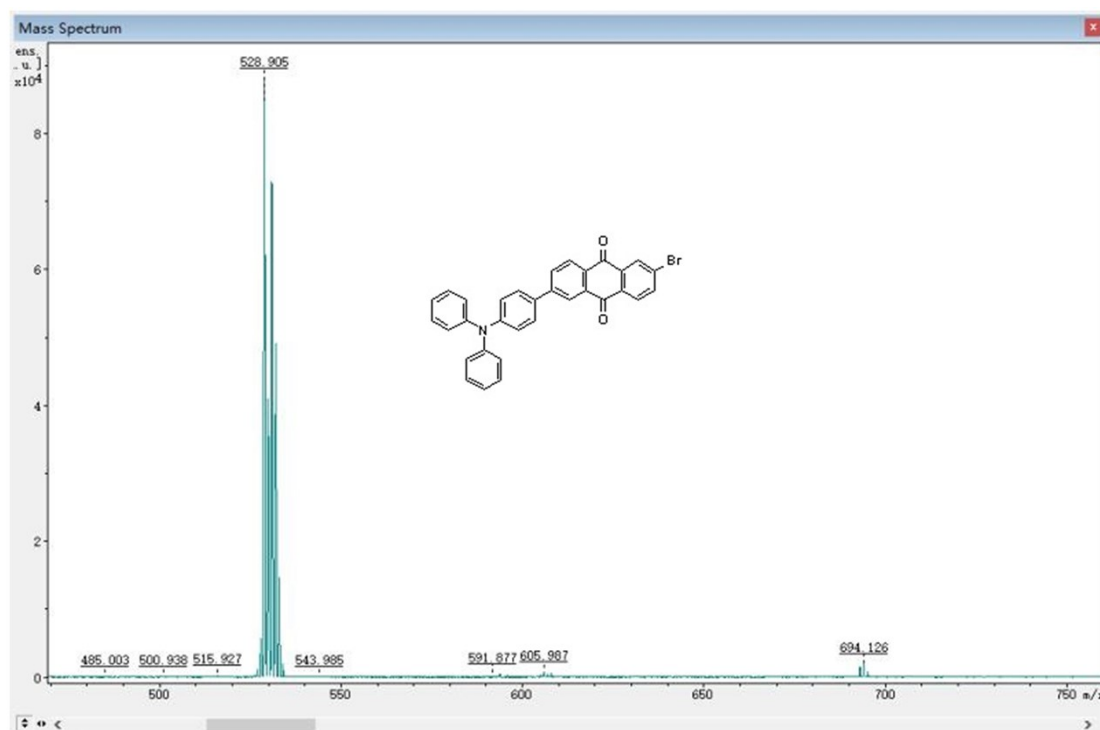

Figure S1. TOF-MS spectrum of TPA-AQ-Br.
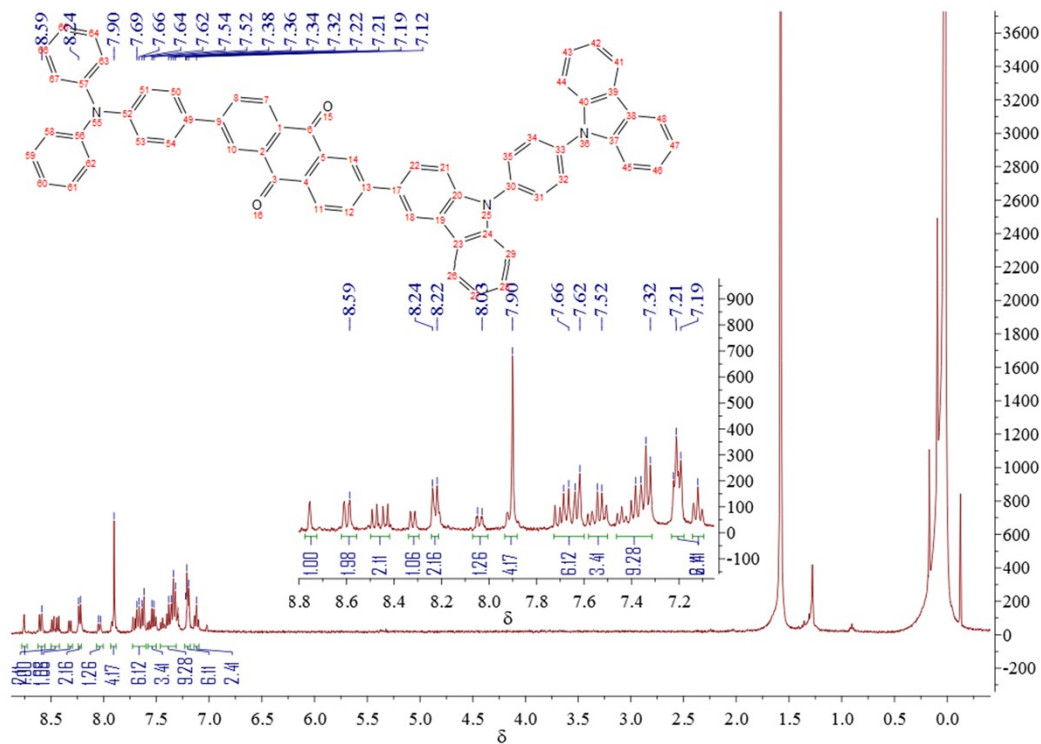
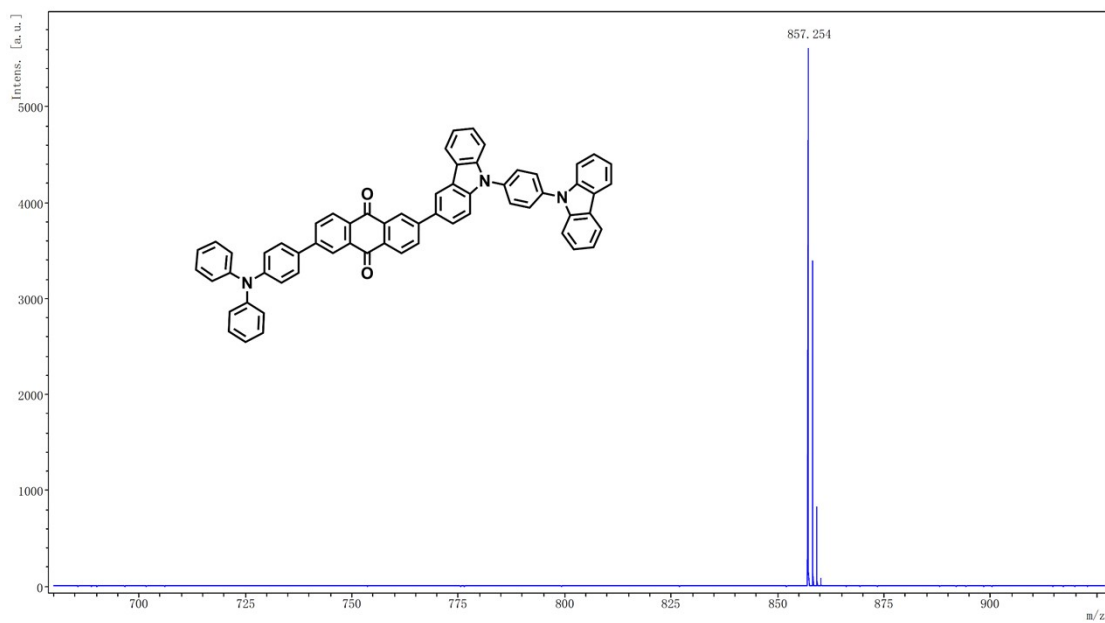**Figure S2**. ^{1}H NMR spectrum of **TPA-AQ-DCP.**

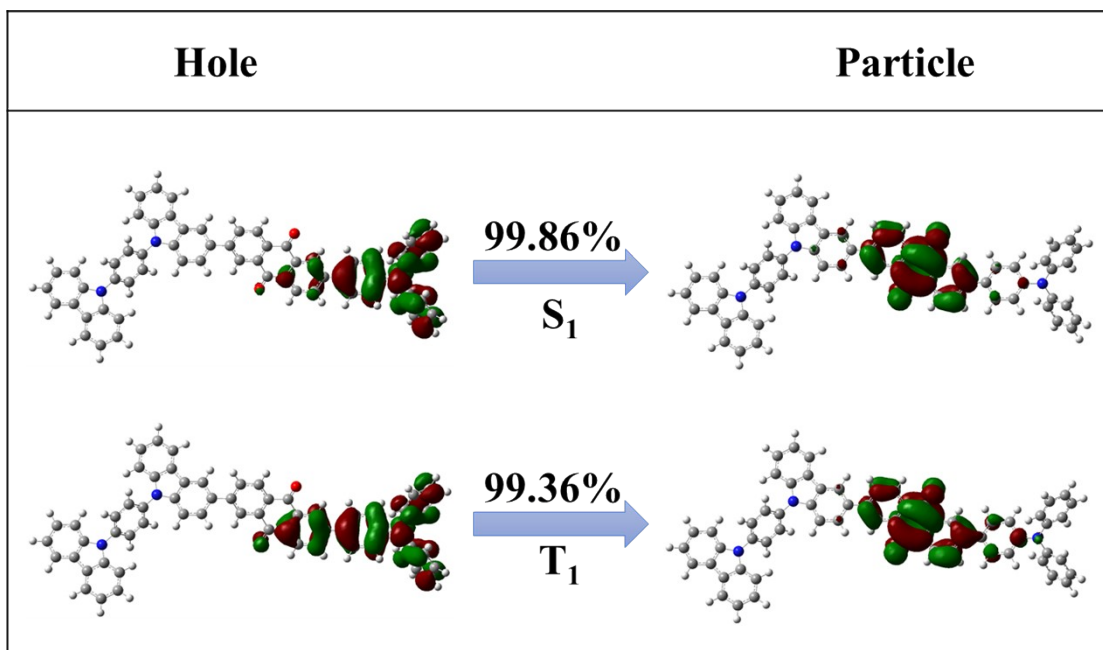**Figure S3.** TOF-MS spectrum of **TPA-AQ-DCP.**

Figure S4. Natural transition orbital (NTO) analysis for **TPA-AQ-DCP**.

Table S1. Results of TD-DFT calculation of **TPA-AQ-DCP** (B3LYP/6-31G(d,p)-GD3 level).

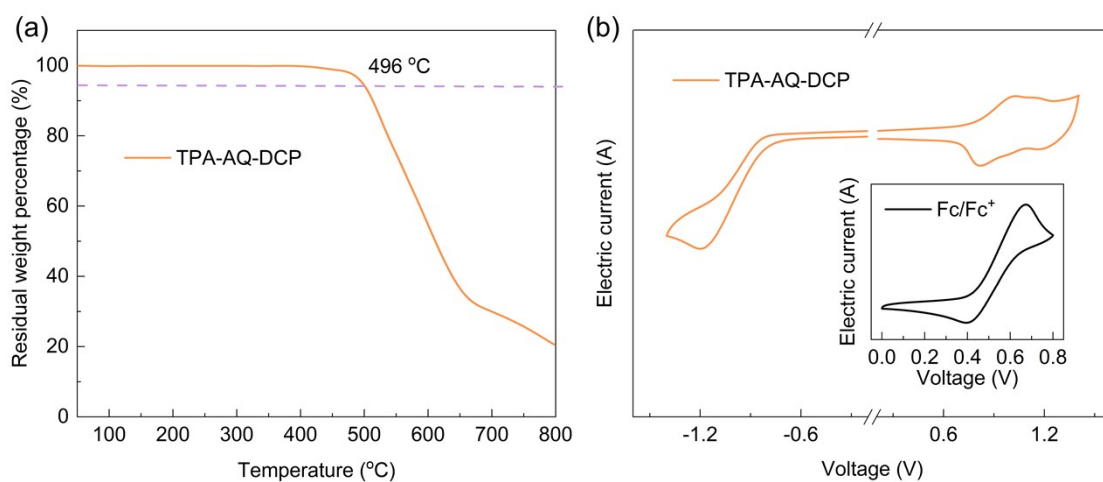| Compound	S_1 [eV]	T_1 [eV]	ΔE_{ST} [eV]	HOMO [eV]	LUMO [eV]	$f(S_0{\rightarrow}S_1)$
TPA-AQ-DCP	2.1420	1.9571	0.1849	-5.0768	-2.6221	0.1620

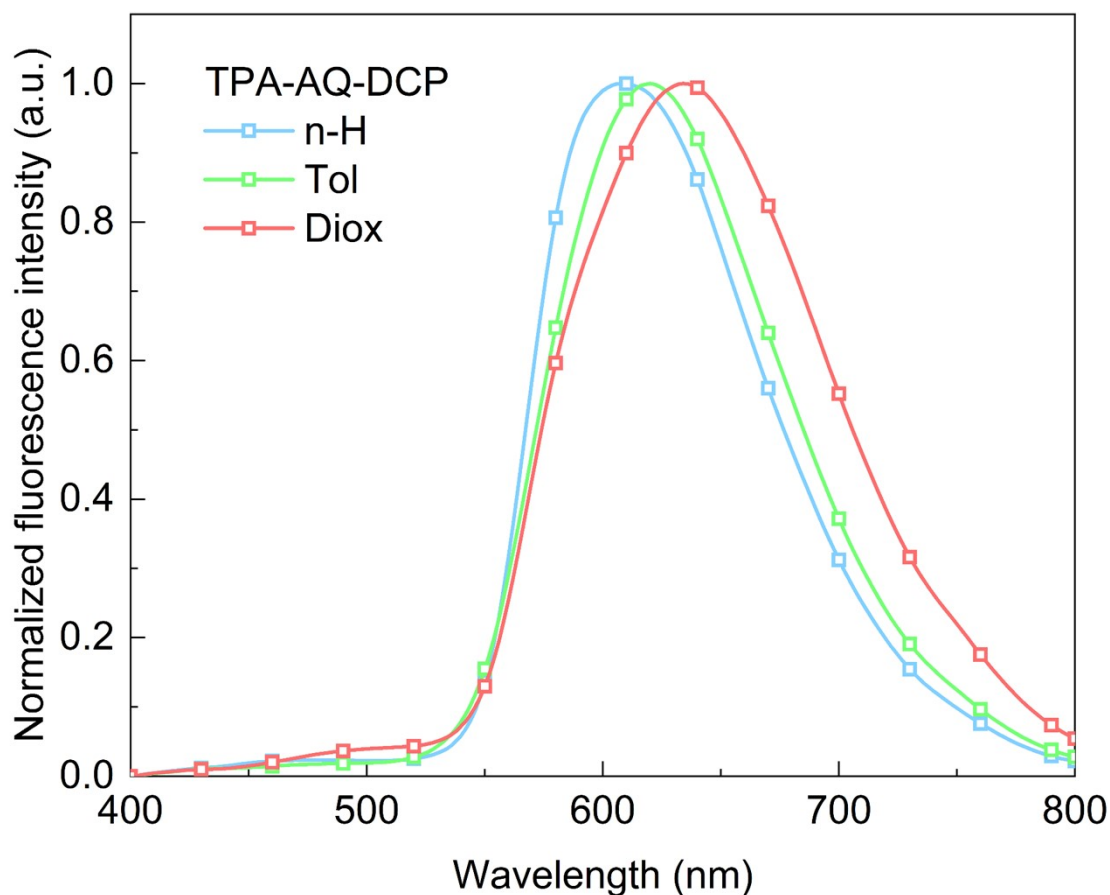**Figure S5.** (a) TGA curves and (b) cyclic voltammetry curves of **TPA-AQ-DCP**.

6

Figure S6. Emission spectra of **TPA-AQ-DCP** in different solvents.

Table S2. Photophysical characteristics of **TPA-AQ-DCP**.

film	Φ_p [%][b]	Φ_d [%][b]	τ_p [ns][c]	τ_d [µs][c]	k_r [10^6 s^{-1}][d]	k_{nr} [10^6 s^{-1}][e]	k_{ISC} [10^6 s^{-1}][f]	k_{RISC} [10^6 s^{-1}][g]
TPA-AQ-DCP[a]	72	7	10.90	6.94	65.99	17.54	8.21	0.16

[a] The doped film is 30 wt% **TPA-AQ-DCP**-doped CBP. [b] Quantum yields for prompt fluorescence (Φ_p) and delayed fluorescence (Φ_d) for the doped film, $\Phi_p + \Phi_d = \Phi_{PL}$. [c] Lifetime of the prompt component (τ_p) and delayed component (τ_d) as determined from the transient PL. [d] Radiative rate constants of S$_1$, $k_r = \Phi_p/\tau_p + \Phi_d/\tau_d$. [e] Nonradiative rate constants of S$_1$, $k_{nr} = k_r(1 - \Phi_{PL})/\Phi_{PL}$. [f] Rate constants for ISC (S$_1 \rightarrow$ T$_1$), $k_{ISC} = k_p - k_r - k_{nr}$. [g] Rate constants for RISC (T$_1 \rightarrow$ S$_1$), $k_{RISC} = k_p k_d/k_{ISC} \cdot \Phi_d/\Phi_p$.
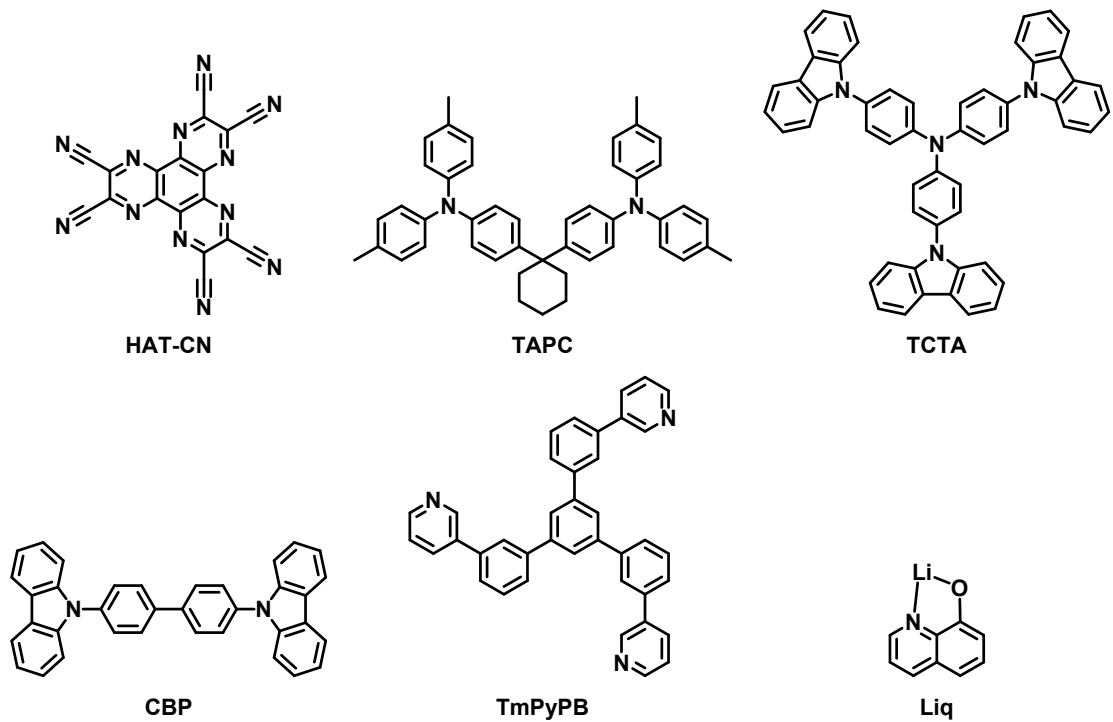
Figure S7. The molecular structure of the related organic materials used in OLEDs.
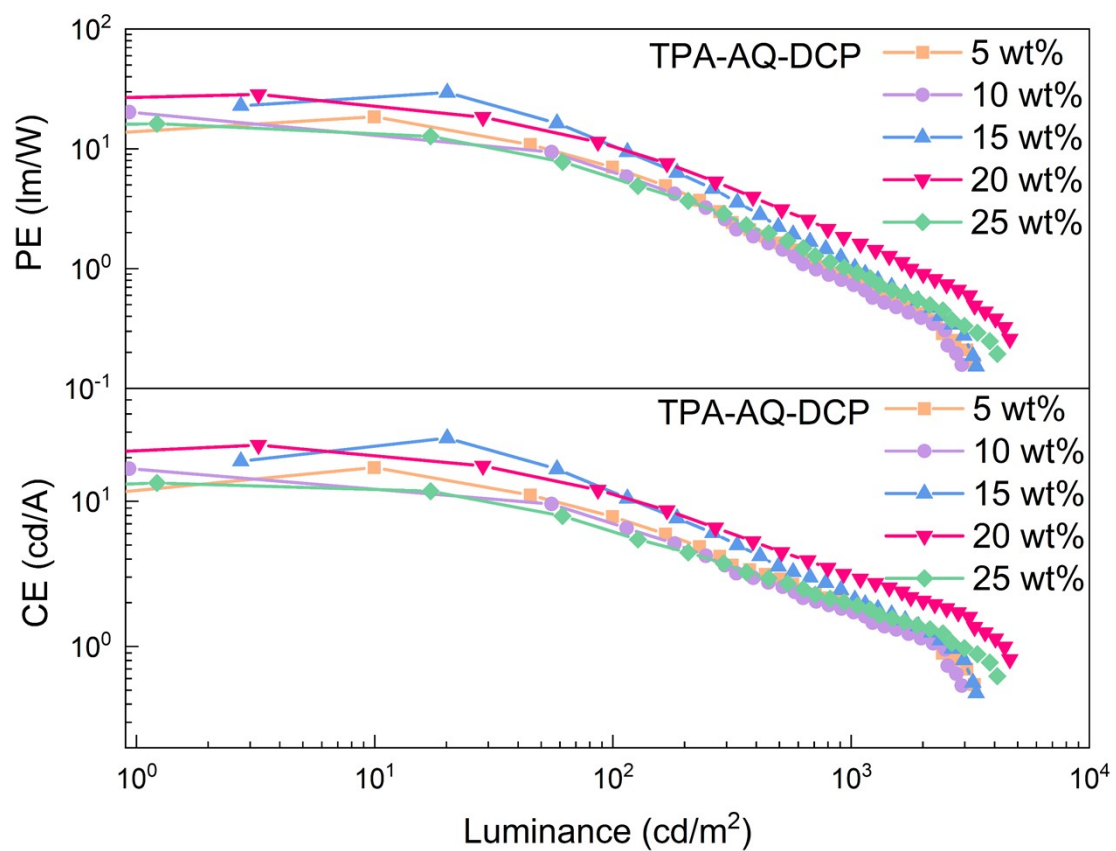

Figure S8. PE and CE as a function of luminance for **TPA-AQ-DCP**-based OLEDs.
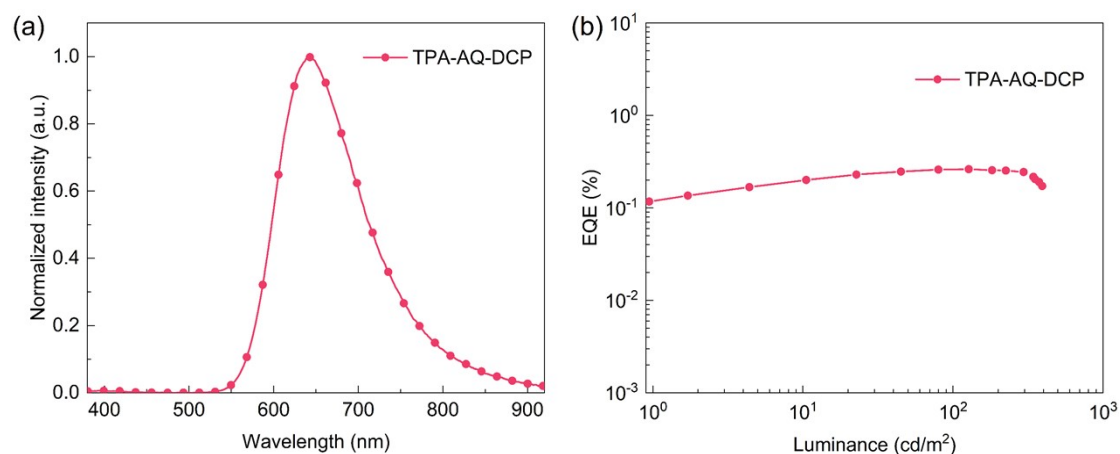
Figure S9. EL performances of TPA-AQ-DCP-based non-doped OLED device: (a) Normalized EL spectra; (b) EQE versus luminance curve.

Table S3. Summary of the EL performance of **TPA-AQ-DCP**-based non-doped OLED device.

Emitter	V_{on}[a]	L_{max}[b]	EQE[c]	CE[c]	PE[c]	λ_{EL}[d]	CIE[d]
	[V]	[cd m^{-2}]	[%]	[cd A^{-1}]	[lm W^{-1}]	[nm]	(x,y)
TPA-AQ-DCP	6.5	393	0.26/0.24	0.19/0.18	0.06/0.05	643	(0.64, 0.35)

[a] Turn-on voltage at 1 cd m^{-2}. [b] Maximum luminance. [c] EQE, CE and PE at maximum and 300 cd m^{-2}, respectively. [d] EL peak and CIE coordinates were recorded at 300 cd m^{-2}.